Bioconjugate Chemistry

Article

pubs.acs.org/bc

Novel Monodisperse PEGtide Dendrons: Design, Fabrication, and Evaluation of Mannose Receptor-Mediated Macrophage Targeting

Jieming Gao,[†] Peiming Chen,[†] Yashveer Singh,[‡] Xiaoping Zhang,[†] Zoltan Szekely,[†] Stanley Stein,[†] and Patrick J. Sinko*[,†]

[†]Department of Pharmaceutics, Ernest Mario School of Pharmacy, Rutgers, The State University of New Jersey, Piscataway, New Jersey 08854, United States

[‡]Department of Chemistry, Indian Institute of Technology Ropar, Nangal Road, Rupnagar, Punjab, 140001, India

Supporting Information

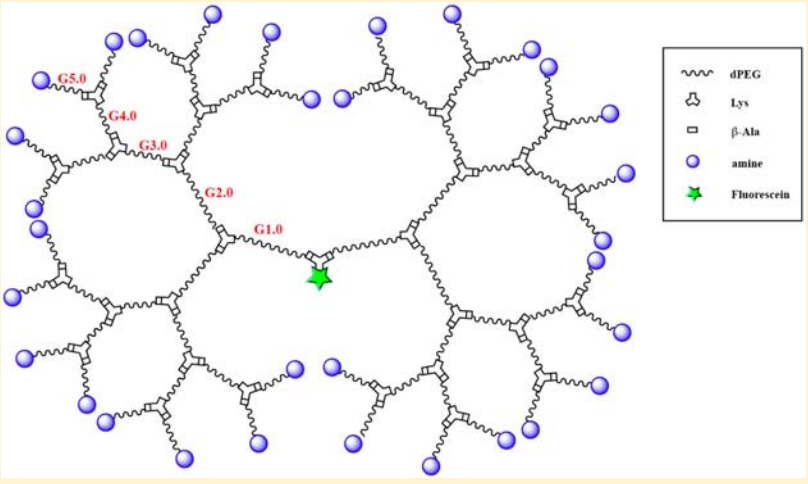

ABSTRACT: Novel PEGtide dendrons of generations 1 through 5 (G1.0−5.0) containing alternating discrete poly(ethylene glycol) (dPEG) and amino acid/peptide moieties were designed and developed. To demonstrate their targeting utility as nanocarriers, PEGtide dendrons functionalized with mannose residues were developed and evaluated for macrophage targeting. PEGtide dendrons were synthesized using 9-fluorenylmethyloxycarbonyl (Fmoc) solid-phase peptide synthesis (SPPS) protocols. The *N*-α-Fmoc-*N*-ε-(5-carboxyfluorescein)-L-lysine (Fmoc-Lys(5-FAM)-OH) and monodisperse Fmoc-dPEG$_6$-OH were sequentially coupled to Fmoc-β-Ala-resin to obtain the resin-bound intermediate Fmoc-dPEG$_6$-Lys(5-FAM)-β-Ala (**1**). G1.0 dendrons were obtained by sequentially coupling Fmoc-Lys(Fmoc)-OH, Fmoc-β-Ala-OH, and Fmoc-dPEG$_6$-OH to **1**. Dendrons of higher generation, G2.0−5.0, were obtained by repeating the coupling cycles used for the synthesis of G1.0. Dendrons containing eight mannose residues (G3.0-mannose$_8$) were developed for mannose receptor (MR) mediated macrophage targeting by conjugating α-D-mannopyranosylphenyl isothiocyanate to G3.0 dendrons. In the present study PEGtide dendrons up to G5.0 were synthesized. The molecular weights of the dendrons determined by MALDI-TOF were in agreement with calculated values. The hydrodynamic diameters measured using dynamic light scattering (DLS) ranged from 1 to 8 nm. Cell viability in the presence of G3.0 and G3.0-mannose$_8$ was assessed using the 3-(4,5-dimethylthiazol-2-yl)-2,5-diphenyltetrazolium bromide (MTT) assay and was found to be statistically indistinguishable from that of untreated cells. G3.0-mannose$_8$ exhibited 12-fold higher uptake than unmodified G3.0 control dendrons in MR-expressing J774.E murine macrophage-like cells. Uptake was nearly completely inhibited in the presence of 10 mg/mL mannan, a mannose analogue and known MR substrate. Confocal microscopy studies demonstrated the presence of significant intracellular punctate fluorescence colocalized with a fluid endocytosis marker with little surface fluorescence in cells incubated with G3.0-mannose$_8$. No significant cell-associated fluorescence was observed in cells incubated with G3.0 dendrons that did not contain the targeting ligand mannose. The current studies suggest that PEGtide dendrons could be useful as nanocarriers in drug delivery and imaging applications.

INTRODUCTION

Dendrimers and dendrons have generated tremendous interest as nanocarriers for various drug delivery applications.[1] Dendrimers and dendrons possess highly branched well-defined three-dimensional structures with three main structural

Received: January 9, 2013
Revised: June 16, 2013
Published: June 29, 2013

ACS Publications © 2013 American Chemical Society

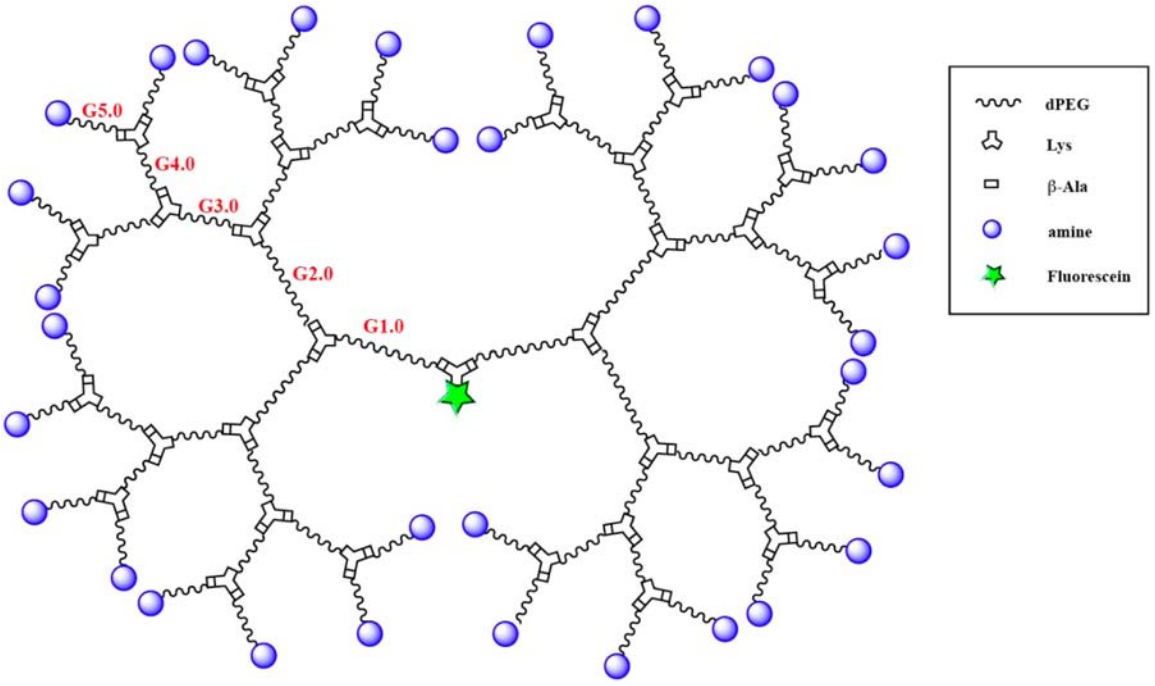

Figure 1. Representative structure of PEGtide dendron, G5.0, containing alternating discrete poly(ethylene glycol) (MW = 264.16 Da) and dipeptide (lysine-β-alanine).

components: the core, the interior, and the shell (surface). The core affects the three-dimensional shape of dendrimers and dendrons, whereas the interior influences host−guest interactions. The surface, on the other hand, can be further modified with drugs, diagnostics, or targeting moieties.[2] Dendrimers are prepared using either divergent or convergent strategies.[3,4] In a divergent approach,[3,5,6] the synthesis proceeds outward from the multifunctional core to the surface, whereas in a convergent approach,[4] dendrimer synthesis proceeds inward by anchoring dendrons to a multifunctional core.

Vögtle and co-workers reported the first synthesis of a dendrimer-like structure, polypropylenimine (PPI), in 1978,[5] and Tomalia [7] and Newkome [3] suggested the term "dendrimer" for such structures in 1985. Several dendritic structures have been developed over the years, and some common examples are polyamidoamine (PAMAM), poly(L-lysine) (PLL), polyamide, polyester (PGLSA-OH), polypropylenimine (PPI), and poly(2,2-bis(hydroxymethyl)propionic acid (bis-MPA).[2] The PAMAM dendrimers, developed by Tomalia and co-workers,[8] are possibly the most extensively investigated dendrimers for drug delivery, imaging, and tissue engineering applications.[2,9] In 1993, Haensler et al. used a complex of PAMAM-G6.0 dendrimer with luciferase gene for high efficiency transfection in cells.[10] In 2006, Majoros et al. designed a multifunctional G5.0-PAMAM dendrimer conjugated to fluorescein, folic acid, and paclitaxel to combine imaging, drug targeting, and therapeutics in one system for tumor therapy.[11] Besides PAMAM, other dendrimers have also been investigated. Luo et al. developed arginine functionalized peptide dendrimers complexed with plasmid DNA for transfection. They showed that this form of dendrimer exhibited high transfection efficiency on all studied cell lines.[12] Similarly, Chisholm et al. showed that a PPI dendrimer complexed to DNA exhibit highly selective tumor distribution and transfection efficiency in mice after intravenous administration.[13]

However, dendrimers are not without limitations. Studies have shown that dendrimers display concentration and generation-dependent cytotoxicities.[14,15] Mukherjee et al. demonstrated that PAMAM dendrimers cause production of reactive oxygen species (ROS), oxidative stress, apoptosis, and DNA damage in mitochondria.[14] Jain et al. conclusively showed that the dendrimer toxicity arises from interactions of the positively charged dendrimer surface with negatively charged biological membranes, leading to membrane disruption via nanohole formation, membrane thinning, and erosion.[16]

Biodegradable dendritic structures (also called self-immolative, cascade-release, and geometrically disassembled) have been developed to overcome toxicity concerns.[17] Shabat,[18] de Groot,[19] and McGrath[20] have developed several dendritic structures containing a trigger unit to cause the degradation of dendrimers into its building blocks.

Incorporation of polyethylene glycol (PEG) moieties into the dendrimer structure has also been used to overcome dendrimer toxicity.[21−23] Fréchet and co-workers developed a variety of core functionalized PEGylated polyester dendrimers to carry up to eight solubilizing groups along with another eight groups in dendritic core for further modification with drug/imaging agents.[24] PEGylated dendrimers showed longer circulation half-life and high accumulation in tumors along with fewer side effects to healthy organs.

The PEG moieties are usually incorporated at the surface or in the core because dendrimer toxicity arises mainly from the core chemistry and is strongly influenced by surface functionalities.[25] However, such strategies have limitations, as they completely ignore biocompatibility concerns arising from the interior layer of dendrimers. Another concern with the use of PEGs, particularly of high molecular weight, is their polydispersity, which is rarely below 1.01, which induces structural heterogeneity in the dendritic structure especially for higher generation dendrimers. To retain the structural homogeneity in PEGylated dendrimers, a few groups have

developed dendrimers incorporating oligoethylene glycol (OEG) based on solution-phase synthesis. This is usually accompanied by tedious purification and is generally limited to low generation dendrimers (G of ≤3).[26,27] Berna et al. synthesized a lower generation (G2.0) dendron/dendrimer containing alternate OEG units and Oregon green dye and demonstrated their efficient internalization by ECV304 cells.[27]

In the present study, an alternative approach for designing and synthesizing biocompatible, biodegradable dendrons of higher generation is reported. Because of the discrete poly(ethylene glycol) (dPEG) building blocks used, a new family of dendrons of superior monodispersity is described. Novel PEGtide dendrons of generation G1.0−5.0, containing alternating monodisperse dPEG and dipeptide Lys-β-Ala, were designed, synthesized, and characterized (Figure 1). The design used in the present work has distinct advantages. It involves incorporation of biocompatible dPEG moieties throughout the dendron, contrary to current strategies where PEGylation is restricted to either the core or surface. It employs dPEGs that lead to the formation of dendrons with no PEG-introduced structural heterogeneity, which is commonly observed in PEG derivatives. Dendron synthesis was achieved using 9-fluorenylmethyloxycarbonyl (Fmoc) solid-phase peptide synthesis (SPPS) protocols, which has the benefit of higher coupling efficiency, automation, and ease of purification. In addition, the convergent synthesis approach allows for precise control of surface targeting ligand spacing, flexibility, and copy number. In addition to dendrons, a G3.0 dendron containing eight mannose residues (G3.0-mannose$_8$) was developed to assess the mannose receptor-mediated macrophage targeting. The G3.0-mannose$_8$ exhibited higher macrophage uptake (12-fold) than unmodified G3.0 dendrons.

MATERIALS AND METHODS

Materials. Fmoc-*N*-amido-dPEG$_6$ acid (MW = 575.65 Da, Fmoc-dPEG$_6$-OH) was purchased from Quanta Biodesign Ltd. (Powell, OH). Fmoc-β-Ala-Wang resin, Fmoc-Lys(Fmoc)-OH, Fmoc-β-Ala-OH, benzotriazole-1-yl-oxy-tris-pyrrolidinophosphonium hexafluorophosphate (PyBOP) were purchased from EMD Chemicals (Gibbstown, NJ). *N*-α-Fmoc-*N*-ε-(5-carboxyfluorescein)-L-lysine (Fmoc-Lys(5-FAM)-OH) and 4″,6-diamidino-2-phenylindole, dihydrochloride (DAPI) were purchased from Anaspec (Fremont, CA). 1-Hydroxybenzotrizole (HOBt) was purchased from Chem-Impex International (Wood Dale, IL). Piperidine, α-D-mannopyranosylphenyl isothiocyanate, triisopropylsilane, sinapinic acid, and 3-(4,5-dimethylthiazol-2-yl)-2,5-diphenyltetrazolium bromide (MTT) were purchased from Sigma-Aldrich (St. Louis, MO). *N*,*N*-Dimethylformamide (DMF), acetic anhydride, *N*,*N*-diisopropylethylamine (DIPEA) were purchased from Acros Organics (Morris Plains, NJ). Trifluoroacetic acid (TFA) was purchased from Fisher Scientific (Pittsburgh, PA). Diethyl ether was purchased from Honeywell Brudick & Jackson (Muskegon, MI), and PD-10 column was purchased from GE Healthcare (Piscataway, NJ). The J774.E murine macrophage cell was a donation from Dr. Philip D. Stahl, Washington University (St. Louis, MO). The U937 cell line was obtained from American Type of Tissue Culture Collection (Manassas, VA). Chambered coverglass (Lab-Tek II) was obtained from Thermo Scientific (Rochester, NY). Hanks' balanced salt solution (HBSS), RPMI-1640 medium and all other cell culture reagents, rhodamine B-labeled dextran (MW = 10 000 Da), and Dulbecco's phosphate buffered saline (DPBS) were purchased from Invitrogen (Carlsbad, CA). All solvents were reagent grade and used as obtained. Chromatography grade solvents were used for HPLC.

PEGtide dendrons were purified on an Alliance reverse-phase high-performance liquid chromatography (RP-HPLC) system (Waters, MA) using a Symmetry C18 column (4.6 mm × 150 mm, 100 Å, particle size 5 μm). The following mobile phase was used: solvent A, 0.05% aqueous TFA; solvent B, acetonitrile containing 0.05% TFA. A linear gradient of 5−30% of B was applied for 60 min at a flow rate of 1 mL/min. The UV absorptions were monitored at 220 and 250 nm, whereas the fluorescence detector was set with excitation and emission wavelengths of 492 and 518 nm, respectively. The dendrons and their derivatives were quantified on a F-7000 fluorescence spectrophotometer (HITACHI, Japan). Mass spectra were acquired on an ABI-MDS SCIEX 4800 matrix-assisted laser desorption/ionization time-of-flight (MALDI-TOF/TOF) mass spectrometer (AB Sciex, Foster City, CA). Sample solutions (2 μL) were mixed with matrix solution (20 μL, 20 mg/mL sinapinic acid in 50% aqueous acetonitrile containing 0.1% TFA). This mixture (1 μL) was spotted onto a sample holder and dried under a gentle stream of argon at room temperature. All spectra were recorded in positive mode using a linear acquisition method. The dynamic light scattering (DLS) measurements were performed on a Zetasizer Nano ZS (Malvern, U.K.) with a He−Ne laser (λ = 633 nm) as the incident beam. Samples were dissolved in Millipore water (pH 7, 1 mg/mL) and filtered through 0.22 μm filters (EMD Millipore, MA).

Synthesis and Characterization of PEGtide Dendrons. *β-Ala-Lys(5-FAM)-dPEG$_6$-Fmoc (1).* The derivative **1** was synthesized on Fmoc-β-Ala-Wang resin (loading capacity, 0.36 mmol/g). The Wang resin (0.1 g) was swollen with DMF in PD-10 column for 1 h, prior to coupling. The N-terminal Fmoc group was removed using piperidine/DMF (1:4 v/v, 2 × 4 mL, 10 min each), followed by washing with DMF. Fmoc-Lys(5-FAM)-OH (7.3 mg, 0.01 mmol) was activated with PyBOP (20.8 mg, 0.04 mmol) and HOBt (5.4 mg, 0.04 mmol) in DMF, mixed with DIPEA (13.2 μL, 0.08 mmol), and transferred to a PD-10 column for coupling. The column was placed on a shaker for 4 h. Next, the resin was washed with DMF and treated with acetic anhydride (24.5 μL, 0.26 mmol) and DIPEA (17.2 μL, 0.10 mmol) in DMF for 0.5 h. Prior to dPEG coupling, the terminal Fmoc group was removed as described earlier. After washing with DMF, Fmoc-dPEG$_6$-OH (23.0 mg, 0.04 mmol), PyBOP (20.8 mg, 0.04 mmol), HOBt (5.4 mg, 0.04 mmol), DIPEA (13.2 μL, 0.08 mmol) in DMF were transferred to a PD-10 column to couple dPEG. The Kaiser test was used to monitor completion of the coupling steps.[28] Finally, the resin was washed with methanol and DCM and then dried in vacuum (108.1 mg of resin was obtained, crude yield of 99%, purity of 99%). MALDI-TOF-MS calculated [M + H$^+$]: 1133.45. Found: 1132.98.

PEGtide Dendrons (G1.0−5.0). G1.0. The Fmoc-Lys-(Fmoc)-OH (23.6 mg, 0.04 mmol), Fmoc-β-Ala-OH (24.9 mg, 0.08 mmol), and Fmoc-dPEG$_6$-OH (46.1 mg, 0.08 mmol), respectively, were coupled to **1** to obtain G1.0. The coupling procedure used was similar to the one described above for the synthesis of **1**. About 4 equiv of PyBOP and HOBt and 8 equiv of DIPEA were used in each coupling step. At the end of the coupling cycles, the terminal Fmoc group was removed using piperidine in DMF. The visual Kaiser test was used to monitor completion of deprotection and coupling steps. The resin was

washed with DMF, DCM, and methanol and dried overnight under vacuum to obtain the resin-bound PEGtide dendron G1.0: 114.8 mg (14.8 mg mass gain, crude yield of 96%, purity of 91%). Finally, the PEGtides were cleaved from support by treatment with a cocktail of TFA/water/triisopropylsilane (TIS) (95/2.5/2.5 v/v/v) for 2 h. The cleavage cocktail was removed under vacuum, and the crude dendrons were purified by HPLC. MALDI-TOF-MS calculated $[M + H^+]$: 1850.94. Found: 1849.72.

G2.0–5.0. The G2.0 PEGtide dendron was obtained from resin-bound Fmoc-protected PEGtide dendron G1.0 (**2**) by using a process similar to the one described earlier for the synthesis of G1.0 dendron. Similarly, G3.0, G4.0, and G5.0 were obtained from resin-bound Fmoc-protected G2.0 (**3**), G3.0 (**4**), and G4.0 (**5**), respectively. The crude yields and purities of support bound PEGtide dendrons G2.0–5.0 were as follows. G2.0: 132.66 mg (32.66 mg mass gain, crude yield of 95%, purity of 87%). G3.0: 165.39 mg (65.39 mg mass gain, crude yield of 91%, purity of 77%). G4.0: 207.40 mg (107.40 mg mass gain, crude yield of 73%, purity of 59%). G5.0: 250.07 mg (150.07 mg mass gain, crude yield of 51%, purity not determined). The crude compounds were purified by HPLC and characterized using MALDI-TOF. G2.0: MALDI-TOF-MS calculated $[M + H^+]$: 3733.06. Found: 3730.31. G3.0: MALDI-TOF-MS calculated $[M + H^+]$: 7495.29. Found: 7486.30. G4.0: MALDI-TOF-MS calculated $[M + H^+]$: 150 22.77. Found: 15022.10. G5.0: MALDI-TOF-MS calculated $[M + H^+]$: 29 709.65; Found: 29 711.08.

Synthesis and Characterization of G3.0-mannose$_8$. The purified PEGtide dendron G3.0 (7.5 mg, 1 μmol) and α-D-mannopyranosylphenyl isothiocyanate (10.0 mg, 32 μmol) were dissolved in sodium carbonate buffer (0.1 M, pH 9.0, 5 mL) and stirred at room temperature for 12 h in dark. The crude product was purified by dialysis (MWCO = 3000 Da) against deionized water for 24 h and lyophilized. The lyophilized PEGtide dendron with eight mannose residues was further purified by HPLC. Crude yield, 8.3 mg (83%). MALDI-TOF-MS calculated $[M + H^+]$: 10 004.90. Found: 10 009.90.

Size Stability Studies. The purified PEGtide dendron G4.0 (1.5 mg, 0.1 μmol) was dissolved in phosphate buffered saline (PBS, 0.1 M, pH 7.0, 1.5 mL) and filtered through PTFE membrane (0.22 μm). The collected filtrate was incubated at 37 °C in an incubator (Forma Scientific Inc., Marietta, OH). An amount of 50 μL of medium was transferred to a cuvette (Hellma GmbH & Co., Germany) at 0, 1, 3, 6, and 10 h for DLS measurement. The stability studies were performed in triplicate.

MTT Assay. The J774.E murine macrophage-like cells were grown as attached cells in a CO_2 incubator with a humidified 5% CO_2 atmosphere at 37 °C. Cells were maintained in RPMI-1640 (GIBCO) containing 10% fetal bovine serum (FBS), 100 U/mL penicillin, and 100 μg/mL streptomycin. For the assay, cells were plated at 2×10^4 (cells/100 μL)/well in a 96-well plate. After 24 h, cells became confluent and were treated with mannan and/or PEGtide dendrons in RPMI-1640 medium containing 10% of fetal bovine serum (thereafter referred to as "medium") under the same conditions as those used for uptake experiments to examine the potential cytotoxicity from these reagents. The cells were preincubated with serum-containing regular medium containing 10 mg/mL mannan or medium without mannan at 37 °C for 1 h, followed by incubation with the same medium containing additionally one of the two dendrons (G3.0 or G3.0-mannose$_8$) at 40 nM for 1 h. After a 1 h incubation at 37 °C in the incubator, the incubation medium was aspirated and 100 μL of fresh medium and 25 μL of MTT (5 mg/mL in PBS) were added to each well, followed by incubation at 37 °C for the next 3 h. The MTT-containing medium was removed and 200 μL of DMSO was added to each well to dissolve the purple crystals. The plate was read for absorbance at 570 nm in a Tecan GENios fluorescent plate reader (Phenix Research Products, Hayward, CA).

Macrophage Uptake Studies. The J774.E murine and the human U937 macrophage-like cells were seeded 2 days before experiment in a 24-well plate at 0.5×10^5 cells/well for quantitative uptake measurement. For confocal microscopy, J774.E cells were seeded 2 days before experiments in a chambered coverglass (Lab-Tek II) at 1.0×10^5 cells/chamber. In the uptake procedure, cells were incubated with 40 nM G3.0 control dendron (without mannose) or G3.0-mannose$_8$ dendron in RPMI-1640 medium containing 10% of fetal bovine serum (medium) at 37 °C for 1 h. For confocal microscopy, the incubation medium included the additional fluid endocytosis marker rhodamine B-labeled dextran (10 000 MW) at 250 μg/mL and the nuclear dye DAPI at 1 μg/mL. For mannan inhibition studies, cells were additionally preincubated with or without 10 mg/mL mannan in medium for 1 h, followed by incubation with dendrons in medium with or without 10 mg/mL mannan. After incubation, the unbound molecules were washed twice with cold DPBS buffer. In preliminary experiments, the incubation buffer was collected after a 1 h incubation and filtered through a Microcon (NMWL, 3 kDa) to demonstrate that no detectable free fluorescence had been produced during the 1 h incubation time. In quantitative uptake experiments, the washed cells were lysed in wells overnight with 150 μL of 1 N NaOH solution per well and neutralized the next day with 150 μL of 1 N HCl solution, resulting in 300 μL of cell lysate/well. An amount of 250 μL of cell lysate was transferred to a well of a black 96-well plate for 5-FAM fluorescence measurement on a Tecan GENios fluorescent plate reader. The total cell-associated fluorescence reading was converted into total cell-associated dendron using two separately established dendron fluorescence standard curves. A small fraction of the lysate (about 50 μL, depending on cell density plated) was used to determine total cellular protein/well by Bradford protein assay.[29] The total cellular protein/well was used to normalize the dendron amount/well to correct well-to-well variation in cell mass. To demonstrate that the total cell-associated dendron was mostly due to internalized fluorescence, as opposed to cell-surface-bound fluorescence, confocal microscopy was carried out in a Z-stack scanning mode on a Leica TCS SP5 confocal microscope (Leica Microsystems Inc., Buffalo Grove, IL). In addition, images of middle sections (0.5 μm thick) of randomly selected cells in different image fields were subject to intracellular fluorescence intensity quantification using the companion software of the confocal microscope. Student's *t* test was used to determine the significance in intracellular fluorescence intensity between selected treatments.

RESULTS

Synthesis and Characterization of PEGtide Dendrons G1.0–5.0. PEGtide dendrons of generations G1.0–5.0 were synthesized by sequentially assembling Fmoc-Lys(Fmoc)-OH, Fmoc-β-Ala-OH, and Fmoc-dPEG$_6$-OH on a solid support. The Fmoc approach of solid-phase peptide synthesis (SPPS)

Scheme 1. Synthesis of PEGtide Dendrons: (A) G1.0 and (B) G2.0−5.0[a]

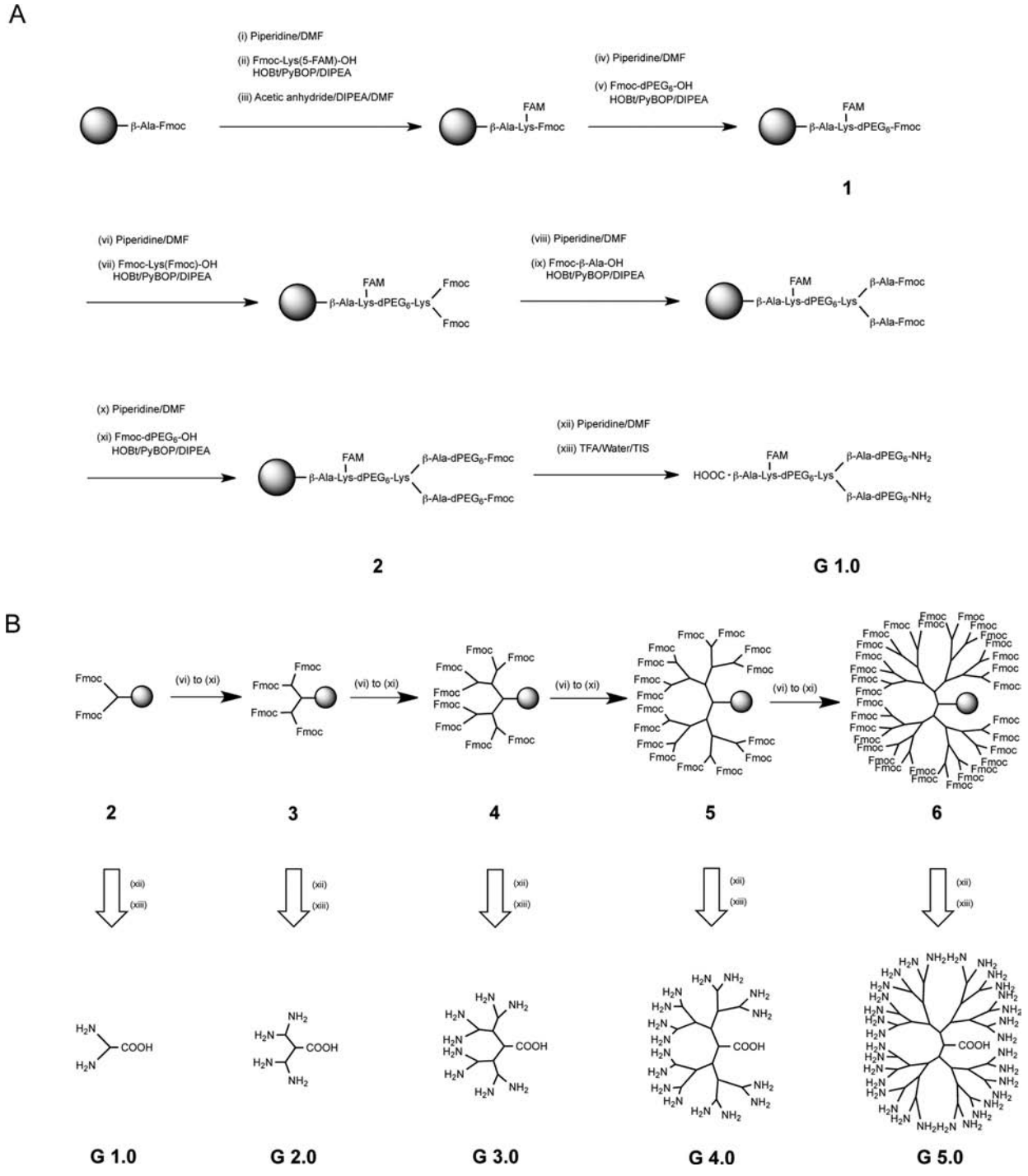

[a]The dendrons were synthesized using Fmoc SPPS using following components: Fmoc-Lys(5-FAM)-OH, Fmoc-Lys(Fmoc)-OH, Fmoc-*β*-Ala-OH, and Fmoc-dPEG$_6$-OH.

and a divergent strategy was used to obtain PEGtide dendrons. Briefly, Fmoc-Lys(5-FAM)-OH and Fmoc-dPEG$_6$-OH were sequentially coupled to Fmoc-*β*-Ala-Wang resin to obtain resin-bound Fmoc-dPEG$_6$-Lys(5-FAM)-*β*-Ala-OH (**1**) (Scheme 1A). 5-FAM-labeled lysine was incorporated in order to detect dendrons in biological assays. The synthesis of PEGtide dendron G1.0 was initiated by coupling Fmoc-Lys(Fmoc)-OH to **1**. In the next step, Fmoc-*β*-Ala-OH was coupled to *α*- and *ε*-amino groups of lysine. Finally, monodisperse Fmoc-dPEG$_6$-OH was coupled to both alanine moieties to obtain resin-bound G1.0 dendrons (**2**). The G1.0 dendrons were obtained after deprotection of terminal Fmoc groups and cleavage from support. Usually a large excess of amino acid/dPEG was used to drive the reaction to completion. HOBt and PyBOP were used for coupling because of their high reactivity and low epimerization of the benzotriazoyl esters of amino acids. Relatively longer coupling times were applied for coupling and deprotection to ensure higher coupling efficiencies.

dx.doi.org/10.1021/bc400011v | *Bioconjugate Chem.* 2013, 24, 1332−1344

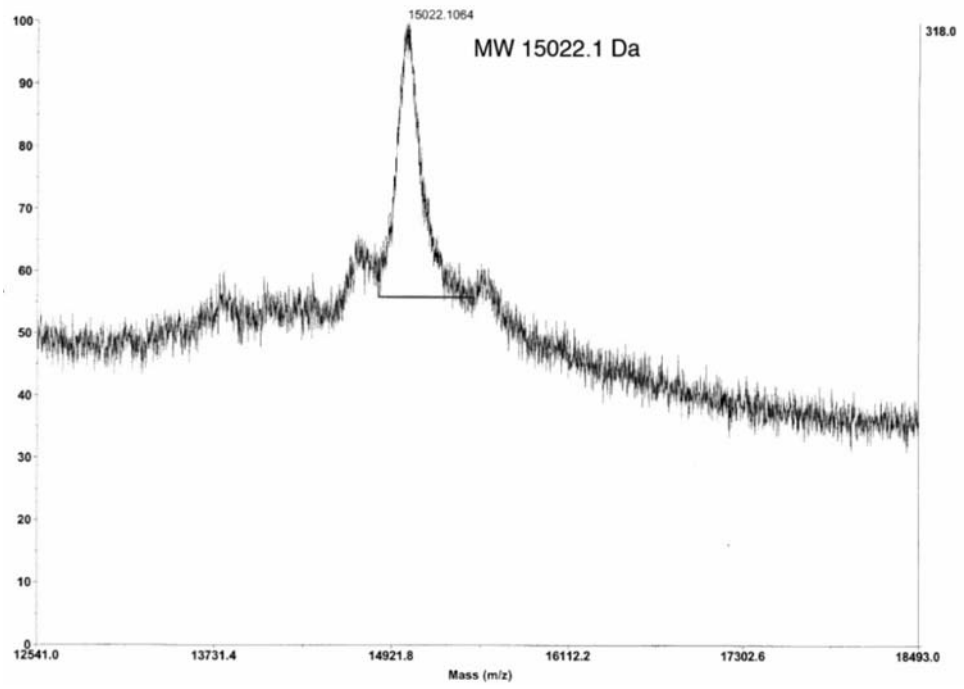

Figure 2. MALDI-TOF mass spectrum of PEGtide dendron G4.0. The observed molecular weight (15 022.1 Da) was in agreement with the calculated molecular weight (15 023.77 Da). The mass spectra for G1.0−3.0 are in the Supporting Information.

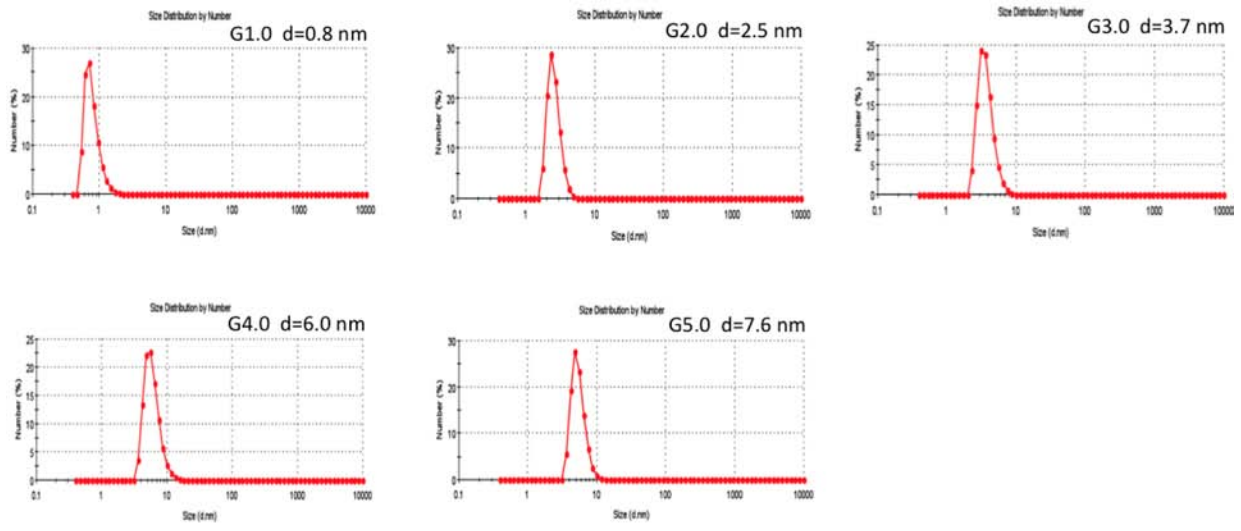

Figure 3. DLS profiles of PEGtide dendrons G1.0−5.0. The hydrodynamic diameters increased with an increase in the generation of dendrons: G1.0, 0.8 nm; G2.0, 2.5 nm; G3.0, 3.7 nm; G4.0, 6.0 nm; G5.0, 7.6 nm.

The higher generation dendrons were synthesized from resin-bound dendrons of previous generation using a procedure described above for the synthesis of G1.0 (Scheme 1B). For example, the dendrons G2.0 were obtained by sequentially coupling Fmoc-Lys(Fmoc)-OH, Fmoc-*β*-Ala-OH, and Fmoc-dPEG$_6$-OH to resin-bound dendron G1.0 (**2**). Similarly, G3.0, G4.0, and G5.0 PEGtide dendrons were obtained from resin-bound G2.0 (**3**), G3.0 (**4**), and G4.0 (**5**) dendrons, respectively. Thus, PEGtide dendrons containing monodisperse dPEG (MW = 264.16 Da) interspersed with dipeptide lysine-*β*-alanine (-Lys-*β*-Ala-) were developed. There are 2, 4, 8, 16, and 32 free terminal amino groups in G1.0, 2.0, 3.0, 4.0, and 5.0 dendrons, respectively, that can be utilized for further modification with drugs, targeting groups, and imaging moieties.

All dendrons were purified by HPLC and characterized using MALDI-TOF and DLS. The purity of PEGtide dendrons was determined using HPLC equipped with a fluorescence detector. Fluorescence detection (excitation and emission at 492 and 518 nm, respectively) was employed because the first lysine incorporated in the dendron core was labeled with 5-FAM. The retention times of PEGtide dendron, G1.0−5.0, were found to be 33.48, 35.05, 37.96, 39.37, and 43.80 min, respectively (see Figure S1 in the Supporting Information). Thus, retention times increased with increasing dendron generation, which was expected, since Baker and co-workers[30] reported similar behavior for amine terminated PAMAM

dx.doi.org/10.1021/bc400011v | *Bioconjugate Chem.* 2013, 24, 1332−1344

Scheme 2. Synthesis of G3.0-Mannose$_8$[a]

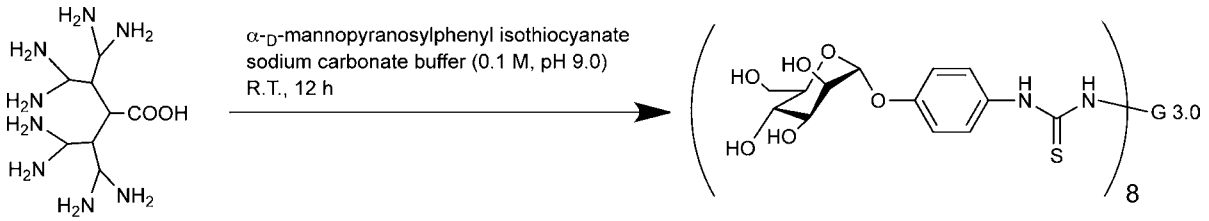

G3.0 G3.0-mannose$_8$

[a]G3.0-mannose$_8$ was obtained by coupling α-D-mannopyranosylphenyl isothiocyanate to free N-terminal of PEGtides G3.0 at room temperature in 0.1 M sodium carbonate buffer (pH 9.0).

dendrimers. The HPLC profiles also demonstrated that dendrons were obtained in high purity. The percentage purities of G1.0−5.0 dendrons were found to be 98.3, 99.0, 96.8, 98.9, and 97.1, respectively (see Figure S1 in the Supporting Information).

The molecular weights of G1.0−5.0 PEGtide dendrons were determined using MALDI-TOF MS. The molecular weights of G1.0, G2.0, G3.0, G4.0, and G5.0 were estimated to be 1849.72, 3730.31, 7486.30, 15 022.10, and 29 711.08 Da, respectively, which were in agreement with calculated values [M + H$^+$] of 1850.94, 3733.06, 7495.29, 15 022.77, and 29 709.65 Da (Figure 2, also see Figure S2 in the Supporting Information; MALDI-TOF mass spectrum for G5.0 is not shown). A representative MALDI-TOF spectrum of purified PEGtide dendron G4.0 is shown in Figure 2. The signal intensity was relatively low when compared to the spectra of low generation dendrons (G1.0−3.0). This is because larger molecules require higher laser power for the desorption and ionization processes.[31] Nevertheless, the ratio of signal to noise was still greater than 10. In each case a single molecular weight peak was obtained, which is uncharacteristic of PEG polymers. This single molecular weight peak is due to the incorporation of monodisperse dPEG in the dendron structure.

The hydrodynamic diameters of G1.0−5.0 PEGtide dendrons were determined using DLS (Figure 3). For all five dendrons a single peak was observed in the particle number figures with a negligible amount of large-sized particles (less than 0.000 001% of the total), indicating that aggregation was insignificant. Unfortunately, the hydrodynamic diameters of G1.0−5.0 PEGtide dendrons in serum-containing medium or pure human serum could not be determined using DLS because serum itself shows up in DLS as a peak that significantly overlaps with the peaks of G1.0−5.0 PEGtide dendrons. A constant 1 mg/mL dendron concentration was used in the DLS analysis for all five dendrons, which translated to molar concentrations ranging from 500 to 30 μM for G1.0−5.0, molar concentrations that were 3 orders of magnitude higher than used in the uptake experiments. Since higher concentration favors aggregation and aggregation was not observed, this suggests that the dendrons at much lower concentrations will be unlikely to aggregate during the 1−2 h uptake time frame of the experiments. The diameters for G1.0, G2.0, G3.0, G4.0, and G5.0 dendrons were determined to be 0.8, 2.5, 3.7, 6.0, 7.6 nm, respectively (Figure 3). Thus, as expected, hydrodynamic diameter increased with increasing dendron generation. The narrow size distribution points to the advantage of using monodisperse dPEG in the dendron structure. Size stability studies of the G4.0 PEGtide in PBS at 37 °C revealed no size changes even after 10 h of incubation (see Figure S6 in the Supporting Information).

Synthesis and Characterization of a Fully Mannosylated, Octavalent PEGtide Dendron (G3.0-Mannose$_8$). To obtain dendrons containing eight copies of mannose, α-D-mannopyranosylphenyl isothiocyanate was coupled to PEGtide G3.0 at room temperature in buffer (pH 9.0). The coupling reaction led to the formation of a stable thiourea linkage (Scheme 2). The G3.0-mannose$_8$ was purified by dialysis (MWCO = 3000 Da) against water. Despite dialysis, the HPLC profile of the conjugate showed the presence of several impurities possibly due to the coupling of varying number of mannose moieties to the G3.0 dendron. Therefore, G3.0-mannose$_8$ was further purified using HPLC and the fraction corresponding to the highest retention time of 75.3 min was collected (see Figure S3 in the Supporting Information). The molecular weight of the purified conjugate was estimated as 10 009.90 Da using MALDI-TOF MS, which was in agreement with the calculated value of 10 004.90 Da [M + H$^+$] and corresponds to the attachment of eight mannose moieties onto the dendron (see Figure S4 in the Supporting Information). The hydrodynamic diameter of the conjugate was estimated to be 4.3 nm by DLS (see Figure S5 in the Supporting Information), which was only slightly higher than PEGtide G3.0 that had a hydrodynamic diameter of 3.7 nm.

Cell viabilities as measured in MTT activity of J774.E murine macrophage-like cells treated with G3.0 or G3.0-mannose$_8$ in the presence or absence of 10 mg/mL mannan are shown in Figure 4. Untreated cells were used as a cell viability reference (100% of MTT activity). The cells were preincubated with serum-containing medium containing 10 mg/mL mannan or serum-containing medium without mannan at 37 °C for 1 h, followed by incubation with the same medium containing additional dendrons at 40 nM for 1 h. The wells of cells were washed and treated with MTT reagent in serum-containing medium for 3 h. The data (Figure 4) showed no statistically significant difference in MTT activity between no treatment and each of the five treatments ($p > 0.05$). The MTT activity was determined under the same conditions as the uptake experiments. Therefore, both the G3.0 and G3.0-mannose$_8$ were not toxic under the uptake experimental conditions in the absence or presence of mannan inhibitor. The MTT assay was also performed using Hanks' buffered saline solution (HBSS) in

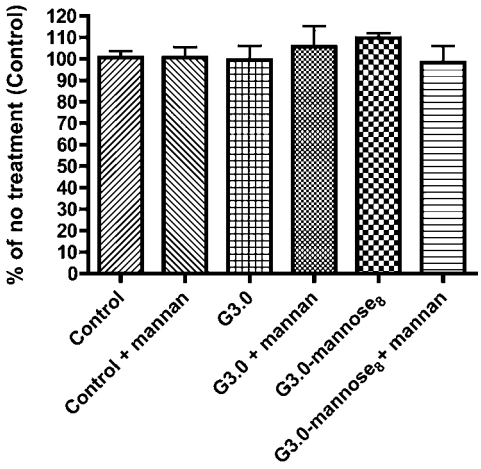

Figure 4. MTT activities of J774.E murine macrophage-like cells without treatment (control) or treated with mannan (control + mannan) or one of the two dendrons (G3.0 and G3.0-mannose$_8$) in the absence or presence of mannan. Control cells were used as cell viability control (100% of MTT activity). The cells were preincubated with serum-containing regular medium containing 10 mg/mL mannan or no mannan at 37 °C for 1 h, followed by incubation with the same medium containing additionally either one of the two dendrons at 40 nM for 1 h. The wells of cells were washed and treated with MTT reagent in regular medium for 3 h. Data are the mean ± sd of three independent experiments with each treatment performed in three wells. Student's *t* test showed no significant difference in MTT activity between no treatment and each of the five treatments ($p > 0.05$).

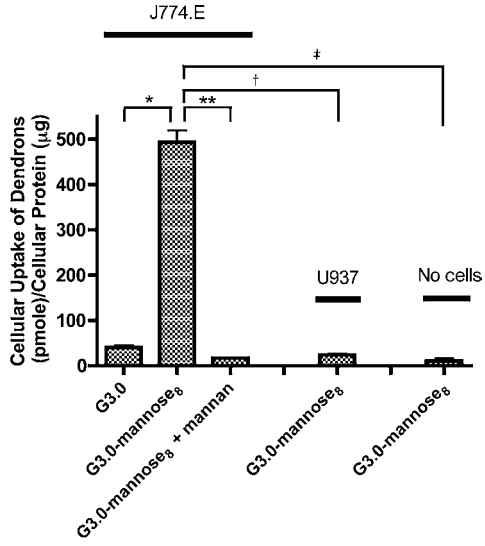

Figure 5. Uptake and mannan inhibition of G3.0-mannose$_8$ in mannose receptor expressing J774.E murine macrophage-like cells and mannose receptor negative U937 cells. The nonmannosylated G3.0 dendron (G3.0) and U937 cells (U937) served as the negative controls, while the blank wells without cells (no cells) indicated the uptake baseline level. The cells were preincubated with or without mannan (10 mg/mL) in serum-containing RPMI-1640 medium for the first hour and then incubated with G3.0 or G3.0-mannose$_8$ (40 nM) in same medium (with or without mannan) at 37 °C for another hour. Dendron cellular uptake was determined by 5-FAM fluorescence intensity against a predetermined standard curve of the labeled dendrons. Uptake was normalized by total cellular protein in each well. Uptake values of G3.0, G3.0-mannose$_8$ without mannan, and G3.0-mannose$_8$ with mannan were 40.7 ± 4.6, 493.5 ± 25.4, and 17.2 ± 0.4 pmol/μg, respectively. Uptake value of G3.0-mannose$_8$ in U937 cells was 24.1 ± 2.9 pmol/μg and that in blank wells was 10.6 ± 5.6 pmol/μg. Data are reported as the mean ± standard deviation from three independent experiments ($n = 12$, (*) $P < 0.05$, (**) $P < 0.01$, (†) $P < 0.05$, (‡) $P < 0.01$).

place of serum-containing medium, and no cytotoxicity was found under this condition either (data not shown).

Macrophage Uptake Studies. The quantitative uptake of G3.0-mannose$_8$ in MR-expressing J774.E murine macrophage-like cells was 493.5 ± 25.4 pmol/μg, whereas that of the nonmannosylated G3.0 (control) was 40.7 ± 4.6 pmol/μg, indicating a 12-fold specificity for G3.0-mannose$_8$ (Figure 5). The mannose analogue mannan at 10 mg/mL (~75 μM) reduced G3.0-mannose$_8$ uptake to 17.2 ± 0.4 pmol/μg (29-fold reduction), further suggesting that the uptake was mannose receptor-mediated (Figure 5). In the literature, mannan was used as a competitive inhibitor of MR ligands at concentrations up to 50 mg/mL.[32] A concentration of 10 mg/mL (or ~75 μM) was used in the current investigation in order to achieve high saturation of the mannose receptor. J774.E murine macrophage-like cells were used because this cell line expresses MR while no human macrophage-like cell lines express detectable MR,[33] including the U937 cell line. As a negative control, U937 cells showed an uptake of 24.1 ± 2.9 pmol/μg that is close to that of G3.0 or that of G3.0-mannose$_8$ in the presence of mannan, once again suggesting the mannose receptor-mediated uptake of G3.0-mannose$_8$. In the uptake experiments, control wells without plated cells were treated the same way as the wells with cells and it was found that no significant G3.0-mannose$_8$ was bound to the plastic surface (Figure 5). We performed these experiments in serum-free medium as well and found no difference in the outcome of the uptake experiments.

Confocal Microscopy. Confocal microscopy was used to assess the cellular localization of the cell-associated dendron fluorescence. The green fluorescence of G3.0-mannose$_8$ was predominantly intracellular with punctate appearance, suggesting little cell surface binding and endocytosis being the cell entry mechanism that results in vesicular (endosomal) localization. The general endocytosis that includes all endocytosis pathways was robust in both G3.0- and G3.0-mannan-treated cells, as the red punctate fluorescence of the fluid endocytosis marker rhodamine B labeled dextran was equally intense (Figure 6). The punctate green fluorescence of G3.0-mannose$_8$ was colocalized with some of, but not all of, the punctate red rhodamine B-dextran (Figure 6, G3.0-mannose$_8$ merged), further suggesting that G3.0-mannose$_8$ was internalized through endocytosis and the endocytosis used only one of the several concurrent endocytosis pathways. In the presence of mannan, the green fluorescence of G3.0-mannose$_8$ was greatly diminished, suggesting MR-mediated and endocytic cell entry (Figure 6). Quantitative intracellular 5-FAM green fluorescence intensity analysis of G3.0 and G3.0-mannose$_8$ dendrons was also performed, in which the green fluorescence of randomly selected individual cells in different fields was quantified using the companion software of the confocal microscope (Figure 7). The fluorescence intensities of G3.0-mannose$_8$, G3.0, and G3.0-mannose$_8$ with mannan were 4.3 ± 1.4, 0.4 ± 0.2, and 0.2 ± 0.1 arbitrary fluorescence units, respectively, representing an 11-fold higher intensity of G3.0-mannose$_8$ over G3.0 and a 22 fold-higher intensity of G3.0-mannose$_8$ in the absence of mannan over that in the presence of mannan. These values are in good agreement with the corresponding values by cellular uptake

dx.doi.org/10.1021/bc400011v | *Bioconjugate Chem.* 2013, 24, 1332−1344

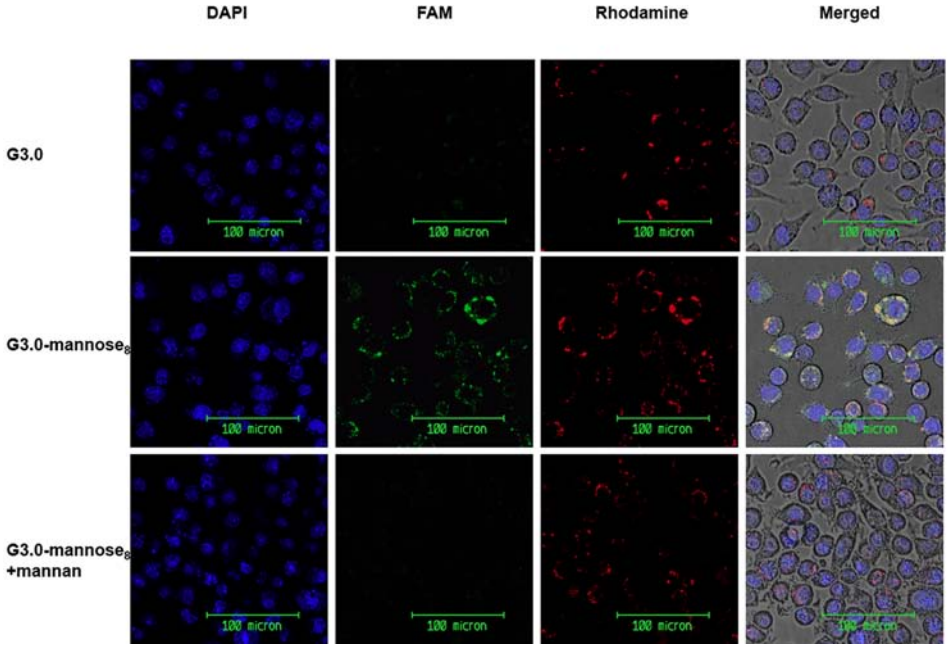

Figure 6. Confocal microscopic images of J774.E murine macrophage-like cells (40× objective) after incubation with 40 nM G3.0 dendrons and G3.0-mannose$_8$ without or with mannan inhibition in RPMI-1640 medium at 37 °C for 1 h and washed three times with Hanks' buffered saline solution. The live cells were scanned in *XYZ* mode at 0.5 μm thickness along the *Z*-axis: DAPI, blue channel scanning; FAM, green channel scanning; rhodamine, red channel scanning; merged, merged images of the blue, the green, the red, and the bright light images of the same field. The yellow-orange color in the merged image of the G3.0-mannose$_8$ treatment indicates colocalization of green and red fluorescence tags.

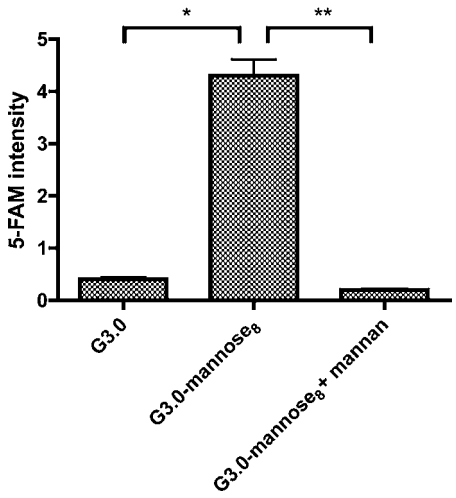

Figure 7. Uptake of dendrons G3.0, G3.0-mannose$_8$ without mannan, and G3.0-mannose$_8$ with mannan in J774.E murine macrophage-like cells. The uptake procedure was the same as described above in Figure 6. Uptake was quantified by 5-FAM green fluorescence of the confocal microscopy images with Leica software (LAS AF Lite, version 2.3.0). The values for G3.0, G3.0-mannose$_8$, and G3.0-mannose$_8$ with mannan were 0.4 ± 0.2, 4.3 ± 1.4, and 0.2 ± 0.1, respectively. Data are reported as the mean ± standard deviation (n = 20 cells for each treatment, (*) $P < 0.05$, (**) $P < 0.05$).

(12-fold and 29-fold, respectively). Therefore, both methods demonstrated mannose receptor-mediated intracellular delivery of the mannosylated G3.0 dendron.

DISCUSSION

Dendrimers and dendrons are considered versatile nanocarriers for drug delivery and imaging applications because they are highly branched and have a well-defined three-dimensional structure.[1,2] The active moieties are either encapsulated into the core/cavities or grafted onto the surfaces. Among different methods for dendrimer synthesis, Tam and co-workers extensively used the SPPS approach for peptide dendrimers synthesis. One typical case was "multiple antigen peptide (MAP)" dendrimers,[34] which have been widely investigated in vaccine and diagnostic research.[35,36] Compared to other synthetic strategies that use costly and time-consuming multistep reactions for the synthesis of dendritic structures, SPPS is more advantageous in its high coupling efficiency and ease of purification.[37] Dendrimers and dendrons are distinct from other nanocarriers in that they possess a tunable structure, an empty intramolecular cavity with relatively high loading capacity, and the potential for a multifunctional surface.[38] In addition, unlike polymers, dendrimers and dendrons are monodisperse, which is an extremely desirable characteristic so far as their synthetic reproducibility and reliability as drug carrier are concerned.[39] Even though promising, dendrimers have been found to exhibit dose- and generation-dependent toxicity in several studies.[14−16] PEGylation has been used to overcome dendrimer cytotoxicity with some success,[22,23,25] but these strategies suffer from PEG polydispersity or restricted PEG modification.

Therefore, current research efforts are focused on improving their drug loading capability, cytotoxicity, and host−guest chemistries. We envisioned an alternative strategy to design higher generation PEGylated dendrons with no structural heterogeneity. A convenient Fmoc-based SPPS approach was employed for PEGtide dendron synthesis. In this approach, monodisperse dPEG was incorporated throughout the dendritic branches rather than restricting it to the core/periphery. Novel PEGtide dendrons of generations G1.0−5.0, containing alternating monodisperse dPEG and dipeptide Lys-β-Ala, were developed using this design (Figure 1). Earlier studies with monodisperse OEG have been limited to low generation

dx.doi.org/10.1021/bc400011v | *Bioconjugate Chem.* 2013, 24, 1332−1344

dendrimers/dendrons (G of ≤3).[26,27] In the present work dendrons have been developed up to the fifth generation (G5.0) (Scheme 1). The dendrons synthesized in this study can be joined together either directly or through a multifunctional core to obtain dendrimers (i.e., through the convergent approach).

The MALDI-TOF mass analyses suggested successful synthesis of PEGtide dendrons (Figure 2, also see Figure S2 in the Supporting Information). MALDI-TOF results also indicated that these dendrons are monodisperse unlike many other PEGylated derivatives. Monodispersity is an important feature for dendron application because it is key to structure−activity relationship studies.[2] For instance, from knowledge of the composition of dendrons, the biological activity can be related to specific aspects of the structure. In gene therapy applications, libraries of monodisperse dendrons with varied size, topology, and transport domain have been explored.[40,41] Using monodispersed structures, Jones compared dendrons of different generations. They found that the hydrophobic domain of the dendrons played a significant role in DNA binding, which was especially significant for low generation dendrons.[41] However, for dendritic structures with branch defects, such as commercial PAMAM or PPI, their inherent structural defects made the evaluation of the structure−activity relationships difficult with respect to gene transfection. The MALDI-TOF mass spectrum confirmed the successful synthesis of PEGtide dendron G5.0 with SPPS strategy (data not shown). However, the SPPS method for G5.0 synthesis faces two limitations in practice. One is the relatively low yield, which is probably related to the steric effects during dendron growth on the solid phase. Another is the difficulty in purification, which is due to the similarity of the hydrophilic properties of the impurities. To resolve these difficulties, a convergent method could be adopted to obtain G5.0 by using purified G4.0. This work is currently being carried out.

All PEGtide dendrons showed adequate water solubility due to the presence of dPEG moieties throughout the dendron structure. Further mass analysis revealed that dPEG constitutes about 50−70% of PEGtide dendron weight in G2.0−5.0 dendrons. Good water solubility is an important feature of PEGtide dendrons, since many nanoparticles and dendrons are poorly soluble. After systemic administration, macrophages, mainly the Kupffer cells in liver, recognize specific opsonin proteins bound to hydrophobic nanoparticles, which leads to macrophage uptake, reticuloendothelial system (RES) accumulation and rapid clearance, and poor biodistribution of nanoparticles. On the other hand, for PEGtide dendrons, multiple layers of highly solvated dPEG should minimize protein absorption and circumvent the rapid clearance from blood circulation. From the point of view of drug loading capability, the high water solubility of PEGtide dendrons provides the opportunity to load more hydrophobic drugs, via either physical encapsulation or chemical bonds conjugation. The MTT assay for G3.0 and G3.0-mannose$_8$ showed no difference in MTT activity whether in the presence or absence of mannan in serum-containing cell culture medium, suggesting that dendrons are not toxic at the concentration tested (40 nM, Figure 4).

The hydrodynamic diameters of G1.0, 2.0, 3.0, 4.0, and 5.0 dendrons measured in PBS using DLS were estimated to be 0.8, 2.5, 3.7, 6.0, and 7.6 nm, respectively (Figure 3). Larger-sized particles accounted for no more than 0.000 01% of total particle number. The filtration process was applied before each size measurement. We also investigated whether the dendrons would aggregate in solution over time. It was observed that the PEGtide dendron G4.0 incubated in PBS (pH 7.0, 37 °C) exhibited no change in hydrodynamic diameter even after 10 h of incubation (see Figure S6 in the Supporting Information). Unfortunately, the stability results in medium containing 10% of FBS by DLS was not absolutely conclusive because of the overlap of serum particle peak with the dendron peak in particle number plots (see Figure S7 in the Supporting Information). Nevertheless, the amount of larger particles in the two test samples was insignifcant. Since it is known that PEGylation shields proteins, nanocarriers, or particles from binding or opsonization by other proteins present in the bloodstream, it is likely that the dendrons are stable in serum as well. Surprisingly PEGtide dendrons with their large surface areas rarely aggregated after filtration. The separation of dendrons in the aqueous environment may be attributed to the high weight percentage of dPEG in PEGtides and possible repulsion between positively charged amine groups on the dendron surface.

Nanocarrier size is critical in many delivery applications because molecules with smaller size (<5 nm) are rapidly eliminated by the kidneys.[39] Our laboratory has used size-based passive accumulation approaches for targeting liver, lungs, and tumors.[42−44] We have also investigated biocompatible PEG nanocarriers for HIV and cancer-targeted drug delivery applications.[45−48] For PEGtide dendrons, one important advantage is their relatively larger size compared to the same generation of other dendrimers or dendrons. This might be attributed to the dPEG moieties, which coordinate two to three water molecules per ethylene oxide unit that increases their apparent molecular weight 5−10 times higher than corresponding globular protein of comparable mass.[49] This large intradendron volume provides the opportunities to load large payloads such as protein, oligonucleotides, and other biofunctional macromolecules. The size of PEGtide dendrons can be further increased by developing higher generation dendrons or by incorporating high molecular weight dPEG units or surface/interior functional moieties. By programming the molecular size of PEGtide dendrons, it should be possible to use these dendrons to passively target tumors by the enhanced permeability and retention (EPR) effect[50] or lymph nodes and deliver antisense oligonucleotides/siRNAs.[51−53]

Mannosylated derivatives selectively bind to mannose receptors expressed on macrophage-like cell lines.[54,55] Since the individual carbohydrate (ligand)−protein (receptor) binding is weak, multivalent interactions are needed to augment ligand−receptor interactions. Biessen et al. developed a series of lysine-based oligomannosides containing two to six terminal α-D-mannose for mannose receptor targeting and found that the affinity of cluster mannosides increased by 10^5 times as the mannose number on cluster glycosides increased from 2 to 6.[56] Since each mannose receptor contains 8 potential mannose-recognition domains, with domain 4 having the highest binding affinity,[56] fluorescently labeled mannosylated PEGtide dendrons of generation G3.0 (G3.0-mannose$_8$), containing eight mannose moieties, were developed for mannose receptor-targeted delivery. G3.0-mannose$_8$ was obtained by conjugating α-D-mannopyranosylphenyl isothiocyanate to G3.0 dendron via thiourea linkage (Scheme 2). As expected, the quantitative uptake studies in mannose receptor expressing J774.E murine macrophage-like cells demonstrated that G3.0-mannose$_8$ has a 12-fold higher specificity for mannose receptor than unmodi-

fied dendrons, G3.0 (Figure 5). These uptake differences between G3.0-mannose$_8$ and G3.0 and between G3.0-mannose$_8$ without and with mannan were further verified by quantitative analysis of confocal images (Figure 7). These differences suggest that cellular entry of G3.0-mannose$_8$ was mannose receptor-mediated (Figure 5). In addition, it was also found that mannosylated dendrons were internalized through endocytosis, using only one of the several concurrent endocytosis pathways.

The most beneficial characteristic of PEGtide dendrons, developed in this work, is their modular design. It is possible to develop dendrons/dendrimers with different structures, including sizes and densities, and multiple functionalities by altering the monodisperse dPEG and amino acid moieties incorporated in dendrons. For example, it is possible to incorporate positively charged amino acids like arginine, lysine, or histidine to complex these dendron with antisense oligonucleotides/siRNA[51−53] for gene delivery applications. The free terminal groups can be protected to mask the positive charges or further modified with drugs, targeting groups, or imaging moieties. PEGtide dendrons are expected to exhibit improved carrier properties in targeted drug delivery and imaging applications.

CONCLUSIONS

PEGtide dendrons of generations G1.0−5.0 were successfully synthesized using a convenient Fmoc-based SPPS approach and characterized using MALDI-TOF MS and DLS. These dendrons can be coupled directly to a multifunctional core to form dendrimers by convergent approach. The dendrons contain monodisperse dPEG alternating with dipeptide Lys-β-Ala, which leads to the formation of monodisperse dendritic structure with no structural heterogeneity. Also, the biocompatible dPEG moieties are present throughout the dendritic structure and not restricted to the core or surface. These dendrons display adequate water solubility and potential good biocompatibility due to the presence of high dPEG content in the dendritic structure, which could be useful in drug delivery applications. The dendrons also contain terminal free amino groups on the surface, which can be protected to mask the terminal positive charges to reduce cytotoxicity or further modified with drugs, targeting groups, or imaging moieties. A G3.0 dendron containing mannose moieties (G3.0-mannose$_8$) showed higher mannose receptor-dependent active uptake than unmodified G3.0 dendrons in macrophages. Thus, PEGtide dendrons developed in this work have the advantage of simple synthesis, easy structural modification, adequate aqueous solubility, and higher biocompatibility. These dendrons, because of their modular design, are expected to be useful as carriers in drug delivery and as molecular tools for imaging applications.

ASSOCIATED CONTENT

Supporting Information

HPLC profiles of G1.0−5.0 PEGtide dendrons, MALDI-TOF mass spectra of G1.0−3.0 dendrons, HPLC profile and MALDI-TOF spectrum of G3.0-mannose$_8$, DLS profile of G3.0-mannose$_8$, size stability evaluation on G4.0, and DLS profiles of cellular culture medium with and without G4.0 dendrons. This material is available free of charge via the Internet at http://pubs.acs.org.

AUTHOR INFORMATION

Corresponding Author

*Phone: 1 848 445 6398. Fax: 1 732 445 4271. E-mail: sinko@rutgers.edu.

Notes

The authors declare no competing financial interest.

ACKNOWLEDGMENTS

This work was supported by NIH Grants R01AI084137, R37AI51214, and R01CA155061. We thank Dr. Philip D. Stahl for providing J774.E murine macrophage cell line and Rutgers University EOSHI/CINJ Analytical Cytometry/Image Analysis Core Facility for assisting with confocal microscopy.

REFERENCES

(1) Oliveira, J. M., Salgado, A. J., Sousa, N., Mano, J. F., and Reis, R. L. (2010) Dendrimers and derivatives as a potential therapeutic tool in regenerative medicine strategies—a review. *Prog. Polym. Sci. 35*, 1163−1194.

(2) Mintzer, M. A., and Grinstaff, M. W. (2011) Biomedical applications of dendrimers: a tutorial. *Chem. Soc. Rev. 40*, 173−190.

(3) Newkome, G. R., Yao, Z. Q., Baker, G. R., and Gupta, V. K. (1985) Micelles. 1. Cascade molecules: a new approach to micelles. A [27]-arborol. *J. Org. Chem. 50*, 2003−2004.

(4) Hawker, C. J., and Frechet, J. M. J. (1990) Preparation of polymers with controlled molecular architecture. A new convergent approach to dendritic macromolecules. *J. Am. Chem. Soc. 112*, 7638−7647.

(5) Egon Buhleier, W. W., and Fritz, Vögtle. (1978) "Cascade"- and "nonskid-chain-like" syntheses of molecular cavity topologies. *Synthesis*, 155−158.

(6) Tomalia, D. A., and Dewald, J. R. (1983) Dense star polymers having core, core branches, terminal groups. U.S. Patent. US4507466.

(7) Tomalia, D. A., Baker, H., Dewald, J., Hall, M., Kallos, G., Martin, S., Roeck, J., Ryder, J., and Smith, P. (1985) A new class of polymers: starburst-dendritic macromolecules. *Polym. J. 17*, 117−132.

(8) Tomalia, D. A., Hall, M., Martin, S., and Smith, P. (1984) A new class of polymers: "starburst-dendritic macromolecules". *Prepr. First Soc. Polym. Sci. Jpn. Int. Polym. Conf.*, 65.

(9) Boas, U., and Heegaard, P. M. (2004) Dendrimers in drug research. *Chem. Soc. Rev. 33*, 43−63.

(10) Haensler, J., and Szoka, F. C. (1993) Polyamidoamine cascade polymers mediate efficient transfection of cells in culture. *Bioconjugate Chem. 4*, 372−379.

(11) Majoros, I. J., Myc, A., Thomas, T., Mehta, C. B., and Baker, J. R. (2006) PAMAM dendrimer-based multifunctional conjugate for cancer therapy: synthesis, characterization, and functionality. *Biomacromolecules 7*, 572−579.

(12) Luo, K., Li, C. X., Li, L., She, W. C., Wang, G., and Gu, Z. W. (2012) Arginine functionalized peptide dendrimers as potential gene delivery vehicles. *Biomaterials 33*, 4917−4927.

(13) Chisholm, E. J., Vassaux, G., Martin-Duque, P., Chevre, R., Lambert, O., Pitard, B., Merron, A., Weeks, M., Burnet, J., Peerlinck, I., Dai, M. S., Alusi, G., Mather, S. J., Bolton, K., Uchegbu, I. F., Schatzlein, A. G., and Baril, P. (2009) Cancer-specific transgene expression mediated by systemic injection of nanoparticles. *Cancer Res. 69*, 2655−2662.

(14) Mukherjee, S. P., Lyng, F. M., Garcia, A., Davoren, M., and Byrne, H. J. (2010) Mechanistic studies of in vitro cytotoxicity of poly(amidoamine) dendrimers in mammalian cells. *Toxicol. Appl. Pharmacol. 248*, 259−268.

(15) Choi, Y. J., Kang, S. J., Kim, Y. J., Lim, Y. B., and Chung, H. W. (2010) Comparative studies on the genotoxicity and cytotoxicity of polymeric gene carriers polyethylenimine (PEI) and polyamidoamine (PAMAM) dendrimer in Jurkat T-cells. *Drug Chem. Toxicol. 33*, 357−366.

(16) Jain, K., Kesharwani, P., Gupta, U., and Jain, N. K. (2010) Dendrimer toxicity: Let's meet the challenge. *Int. J. Pharm. 394*, 122−142.
(17) Amir, R. J., and Shabat, D. (2006) Domino dendrimers. *Adv. Polym. Sci. 192*, 59−93.
(18) Amir, R. J., Pessah, N., Shamis, M., and Shabat, D. (2003) Self-immolative dendrimers. *Angew. Chem., Int. Ed. 42*, 4494−4499.
(19) de Groot, F. M. H., Albrecht, C., Koekkoek, R., Beusker, P. H., and Scheeren, H. W. (2003) "Cascade-release dendrimers" liberate all end groups upon a single triggering event in the dendritic core. *Angew. Chem., Int. Ed. 42*, 4490−4494.
(20) Szalai, M. L., Kevwitch, R. M., and McGrath, D. V. (2003) Geometric disassembly of dendrimers: dendritic amplification. *J. Am. Chem. Soc. 125*, 15688−15689.
(21) Taratula, O., Garbuzenko, O. B., Kirkpatrick, P., Pandya, I., Savla, R., Pozharov, V. P., He, H. X., and Minko, T. (2009) Surface-engineered targeted PPI dendrimer for efficient intracellular and intratumoral siRNA delivery. *J. Controlled Release 140*, 284−293.
(22) He, H., Li, Y., Jia, X. R., Du, J., Ying, X., Lu, W. L., Lou, J. N., and Wei, Y. (2011) PEGylated poly(amidoamine) dendrimer-based dual-targeting carrier for treating brain tumors. *Biomaterials 32*, 478−487.
(23) Yuan, Q. A., Yeudall, W. A., and Yang, H. (2010) PEGylated polyamidoamine dendrimers with bis-aryl hydrazone linkages for enhanced gene delivery. *Biomacromolecules 11*, 1940−1947.
(24) Guillaudeu, S. J., Fox, M. E., Haidar, Y. M., Dy, E. E., Szoka, F. C., and Frechet, J. M. J. (2008) PEGylated dendrimers with core functionality for biological applications. *Bioconjugate Chem. 19*, 461−469.
(25) Gajbhiye, V., Kumar, P. V., Tekade, R. K., and Jain, N. K. (2007) Pharmaceutical and biomedical potential of PEGylated dendrimers. *Curr. Pharm. Des. 13*, 415−429.
(26) Newkome, G. R., Kotta, K. K., Mishra, A., and Moorefield, C. N. (2004) Synthesis of water-soluble, ester-terminated dendrons and dendrimers containing internal PEG linkages. *Macromolecules 37*, 8262−8268.
(27) Berna, M., Dalzoppo, D., Pasut, G., Manunta, M., Izzo, L., Jones, A. T., Duncan, R., and Veronese, F. M. (2006) Novel monodisperse PEG-dendrons as new tools for targeted drug delivery: synthesis, characterization and cellular uptake. *Biomacromolecules 7*, 146−153.
(28) Kaiser, E, C. R., Bossinger, C. D., and Cook, P. I. (1970) Color test for detection of free terminal amino groups in the solid-phase synthesis of peptides. *Anal. Biochem. 34*, 595−598.
(29) Zor, T., and Seliger, Z. (1996) Linearization of the bradford protein assay increases its sensitivity: theoretical and experimental studies. *Anal. Biochem. 236*, 302−308.
(30) Islam, M. T., Shi, X. Y., Balogh, L., and Baker, J. R. (2005) HPLC separation of different generations of poly(amidoamine) dendrimers modified with various terminal groups. *Anal. Chem. 77*, 2063−2070.
(31) Yu, D., Vladimirov, N., and Frechet, J. M. J. (1999) MALDI-TOF in the characterizations of dendritic-linear block copolymers and stars. *Macromolecules 32*, 5186−5192.
(32) Fanibunda, S. E., Modi, D. N., Gokral, J. S., and Bandivdekar, A. H. (2011) HIV gp120 binds to mannose receptor on vaginal epithelial cells and induces production of matrix metalloproteinases. *PLoS One 6*, e28014.
(33) Vigerust, D. J., Vick, S., and Shepherd, V. L. (2012) Characterization of functional mannose receptor in a continuous hybridoma cell line. *BMC Immunol. 13*, 51−63.
(34) Tam, J. P. (1988) Synthetic peptide vaccine design: synthesis and properties of a high-density multiple antigenic peptide system. *Proc. Natl. Acad. Sci. U.S.A. 85*, 5409−5413.
(35) Cubillos, C., de la Torre, B. G., Jakab, A., Clementi, G., Borras, E., Barcena, J., Andreu, D., Sobrino, F., and Blanco, E. (2008) Enhanced mucosal immunoglobulin a response and solid protection against foot-and-mouth disease virus challenge induced by a novel dendrimeric peptide. *J. Virol. 82*, 7223−7230.
(36) Aguilar, R. M., Talamantes, F. J., Bustamante, J. J., Munoz, J., Trevino, L. R., Martinez, A. O., and Haro, L. S. (2009) MAP dendrimer elicits antibodies for detecting rat and mouse GH-binding proteins. *J. Pept. Sci. 15*, 78−88.
(37) Balaji, B. S., Gallazzi, F., Jia, F., and Lewis, M. R. (2006) An efficient, convenient solid-phase synthesis of amino acid-modified peptide nucleic acid monomers and oligomers. *Bioconjugate Chem. 17*, 551−558.
(38) Duncan, R., and Izzo, L. (2005) Dendrimer biocompatibility and toxicity. *Adv. Drug Delivery Rev. 57*, 2215−2237.
(39) Lee, C. C., MacKay, J. A., Frechet, J. M. J., and Szoka, F. C. (2005) Designing dendrimers for biological applications. *Nat. Biotechnol. 23*, 1517−1526.
(40) Delort, E., Nguyen-Trung, N. Q., Darbre, T., and Reymond, J. L. (2006) Synthesis and activity of histidine-containing catalytic peptide dendrimers. *J. Org. Chem. 71*, 4468−4480.
(41) Jones, S. P., Gabrielson, N. P., Wong, C. H., Chow, H. F., Pack, D. W., Posocco, P., Fermeglia, M., Pricl, S., and Smith, D. K. (2011) Hydrophobically modified dendrons: developing structure−activity relationships for DNA binding and gene transfection. *Mol. Pharmaceutics 8*, 416−429.
(42) Kutscher, H. L., Chao, P. Y., Deshmukh, M., Rajan, S. S., Singh, Y., Hu, P. D., Joseph, L. B., Stein, S., Laskin, D. L., and Sinko, P. J. (2010) Enhanced passive pulmonary targeting and retention of PEGylated rigid microparticles in rats. *Int. J. Pharm. 402*, 64−71.
(43) Kutscher, H. L., Chao, P., Deshmukh, M., Singh, Y., Hu, P., Joseph, L. B., Reimer, D. C., Stein, S., Laskin, D. L., and Sinko, P. J. (2010) Threshold size for optimal passive pulmonary targeting and retention of rigid microparticles in rats. *J. Controlled Release 143*, 31−37.
(44) Chao, P. Y., Deshmukh, M., Kutscher, H. L., Gao, D. Y., Rajan, S. S., Hu, P. D., Laskin, D. L., Stein, S., and Sinko, P. J. (2010) Pulmonary targeting microparticulate camptothecin delivery system: anticancer evaluation in a rat orthotopic lung cancer model. *Anti-Cancer Drugs 21*, 65−76.
(45) Paranjpe, P. V., Chen, Y., Kholodovych, V., Welsh, W., Stein, S., and Sinko, P. J. (2004) Tumor-targeted bioconjugate based delivery of camptothecin: design, synthesis and in vitro evaluation. *J. Controlled Release 100*, 275−292.
(46) Wan, L., Pooyan, S., Hu, P., Leibowitz, M. J., Stein, S., and Sinko, P. J. (2007) Peritoneal macrophage uptake, pharmacokinetics and biodistribution of macrophage-targeted PEG-fMLF (*N*-formyl-methionyl-leucyl-phenylalanine) nanocarriers for improving HIV drug delivery. *Pharm. Res. 24*, 2110−2119.
(47) Gao, J. M., Ming, J., He, B., Fan, Y. J., Gu, Z. W., and Zhang, X. D. (2008) Preparation and characterization of novel polymeric micelles for 9-nitro-20(S)-camptothecin delivery. *Eur. J. Pharm. Sci. 34*, 85−93.
(48) Gao, J. M., Ming, J., He, B., Gu, Z. W., and Zhang, X. D. (2008) Controlled release of 9-nitro-20(S)camptothecin from methoxy poly(ethylene glycol)-poly(D,L-lactide) micelles. *Biomed. Mater.* 3, 015013.
(49) Manjula, B. N., Tsai, S., Upadhya, R., Perumalsamy, K., Smith, P. K., Malavalli, A., Vandegriff, K., Winslow, R. M., Intaglietta, M., Prabhakaran, M., Friedman, J. M., and Acharya, A. S. (2003) Site-specific PEGylation of hemoglobin at cys-93(beta): correlation between the colligative properties of the PEGylated protein and the length of the conjugated PEG chain. *Bioconjugate Chem. 14*, 464−472.
(50) Matsumura, Y., and Maeda, H. (1986) A new concept for macromolecular therapeutics in cancer-chemotherapy: mechanism of tumoritropic accumulation of proteins and the antitumor agent smancs. *Cancer Res. 46*, 6387−6392.
(51) Opalinska, J. B., and Gewirtz, A. M. (2002) Nucleic-acid therapeutics: basic principles and recent applications. *Nat. Rev. Drug Discovery 1*, 503−514.
(52) Pack, D. W., Hoffman, A. S., Pun, S., and Stayton, P. S. (2005) Design and development of polymers for gene delivery. *Nat. Rev. Drug Discovery 4*, 581−593.

(53) Whitehead, K. A., Langer, R., and Anderson, D. G. (2009) Knocking down barriers: advances in siRNA delivery. *Nat. Rev. Drug Discovery 8*, 129−138.
(54) Wijagkanalan, W., Kawakami, S., Takenaga, M., Igarashi, R., Yamashita, F., and Hashida, M. (2008) Efficient targeting to alveolar macrophages by intratracheal administration of mannosylated liposomes in rats. *J. Controlled Release 125*, 121−130.
(55) Yeeprae, W., Kawakami, S., Yamashita, F., and Hashida, M. (2006) Effect of mannose density on mannose receptor-mediated cellular uptake of mannosylated O/W emulsions by macrophages. *J. Controlled Release 114*, 193−201.
(56) Biessen, E. A. L., Noorman, F., van Teijlingen, M. E., Kuiper, J., Barrett-Bergshoeff, M., Bijsterbosch, M. K., Rijken, D. C., and van Berkel, T. J. C. (1996) Lysine-based cluster mannosides that inhibit ligand binding to the human mannose receptor at nanomolar concentration. *J. Biol. Chem. 271*, 28024−28030.